On the impact of modelling tension-compression asymmetry on earing and thickness predictions

P.D. Barros, M.C. Oliveira, J.L. Alves & L.F. Menezes

Published online: 31 May 2019.

Submit your article to this journal ⟋

View related articles ⟋

View Crossmark data ⟋

Taylor & Francis
Taylor & Francis Group

Check for updates

RESEARCH ARTICLE

On the impact of modelling tension-compression asymmetry on earing and thickness predictions

P.D. Barros [ID][a], M.C. Oliveira [ID][a], J.L. Alves [ID][b] and L.F. Menezes [ID][a]

[a]CEMMPRE, Department of Mechanical Engineering, University of Coimbra, Coimbra, Portugal; [b]CMEMS, Center for Microelectromechanical Systems Research Unit, University of Minho, Guimarães, Portugal

ABSTRACT

The metallic sheets used in sheet metal forming processes typically exhibit orthotropic behaviour, due to their crystallographic structure and the rolling process from which they are obtained. The yield criteria commonly adopted in the numerical analysis of these processes, assume that the yield surface possesses a point-symmetry with respect to its centre. However, even metallic materials with a cubic structure can present asymmetry between the tensile and the compressive plastic behaviour. Thus, it is important to evaluate the impact of considering the tension-compression asymmetry in the accuracy of the numerical results. The cylindrical cup example is known for being sensitive to both the material yield stresses and *r*-values in-plane directionalities. In this work, the behaviour of a AA2090-T3 aluminium alloy is described with an orthotropic yield criterion that also enables the description of tension-compression asymmetry. The numerical simulations of a cylindrical cup drawing were performed and the main parameters analysed are the earing profile and the thickness distribution, along the rolling and the transverse directions. The comparison of the experimental and numerical results shows that considering the compression yield stresses is critical to obtain accurate predictions, particularly for the thickness distribution.

1. Introduction

Sheet metal forming processes are widely used in the manufacturing industry of metallic sheets, due to the high production rates and minimum material waste. This technological process consists in modifying the original geometry of the material by applying external forces, under a combination of tensile and compressive conditions, which induce plastic deformation of the material. Sheet metal forming processes are designed and optimized virtually using finite element analysis (FEA), consequently decreasing the time-to-market life cycle and allowing notable savings in terms of money, time and effort in the design, production and process set-up of new-formed parts. However, the success of finite elements solvers on the design and optimization of sheet metal-formed parts is strongly dependent on their ability for accurately describing the material's mechanical behaviour.

Metals sheets, due to their crystallographic structure and the rolling process from which are obtained, generally exhibit anisotropy, characterized by the symmetry of their mechanical properties with respect to three orthogonal planes, i.e. orthotropy [1]. Thus, different mechanical behaviours are expected for different loading directions and conditions. Moreover, sheet metal forming processes are carried out with inhomogeneous deformation and under multiaxial strain paths.

In order to describe the elastoplastic response of metal sheets, phenomenological models are commonly used due to their improved computational efficiency when compared with microstructural-based models. When adopting an associated flow rule, the material's orthotropic behaviour is modelled by a yield surface, describing both the yielding and the plastic flow of the material. This dual role of the yield surface requires a particular care and accuracy in its modelling, numerical implementation and in the procedure adopted to perform the parameters identification.

For isotropic materials, Tresca [2] and von Mises [3] yield criteria are the most widely used. The Hill'48 [4] quadratic function was the first proposed for anisotropic materials and it is still the most widely used. Other formulations have been proposed to improve the description of the mechanical behaviour of orthotropic metallic materials, in particular, aluminium and its alloys, since they are prone to present an anisotropic behaviour which cannot be accurately described by quadratic yield criteria [1]. The description of the orthotropic behaviour is critical for an accurate description of the material flow, during the forming process. In fact, several authors refer that an improved modelling of both the materials yield stresses and r-values in-plane directionalities improves the accuracy of the earing profile prediction on the deep drawing of cylindrical cups [5,6].

The anisotropy parameters must be identified enabling the yield criterion to reproduce the materials mechanical behaviour as close as possible. This procedure is typically based on solving an optimization problem, considering the minimization of an error function, which evaluates the difference between the estimated and the experimentally evaluated values. Classical identification methodologies consider the experimental data acquired from experimental tests, characterized for presenting linear strain paths (namely uniaxial tensile, bulge and shear tests). These tests present homogeneous deformation in the measuring region, allowing the estimate of the yield stress and anisotropy coefficient. The uniaxial and shear tests can also be performed using specimens cut in several directions of the sheets plane (generally, 0, 15, 30, 45, 60, 75 and 90 degrees from the rolling direction). More flexible yield functions are commonly characterized for presenting a higher number of anisotropy parameters and, consequently, require a significant number of experimental tests to enable their identification. Also, limiting the characterization of the mechanical behaviour of metal sheets to a restricted number of tests with linear strain paths and homogeneous deformation can lead to a somewhat incomplete characterization of the overall plastic behaviour of the material [7]. Therefore, inverse identification methodologies have also been proposed, trying to explore the information obtained from more complex experimental tests involving non-homogeneous strain fields, to identify only the yield criterion parameters [8] or also the isotropic hardening, using cruciform [9,10] or out-of-plane specimens [11]. Anyhow, due to several experimental limitations, a fundamental problem with the phenomenological approach is that most of the stress space is left unexplored when fitting the parameters of the yield function with either classical or inverse methodologies [12].

In most numerical analysis of sheet metal forming processes, the yield surface is assumed to possess a point-symmetry with respect to its centre, meaning that a stress state and its reverse state have the same absolute value [1]. However, this can be an unrealistic approximation, even for cubic metals (both face centred cubic (FCC) and body centred cubic (BCC)) [13]. Cazacu and Barlat [14] extended the Drucker [15] isotropic yield function to the anisotropic case through invariants generalizing, to enable the description of both the materials anisotropy and the tension-compression asymmetry. Later, Cazacu et al. [16] presented a yield criterion that enables describing also both effects using a linear transformation, with a fourth-order tensor, of the deviatoric stress tensor. This formulation is more flexible, since it enables the adoption of several linear transformations, in order to more accurately capture the material's anisotropic behaviour [17,18]. However, adopting several linear transformations means that the yield surface modelling becomes more complex, due to the higher number of material anisotropy parameters involved, thus requiring a larger set of experimental data.

In order to characterize the metallic sheets mechanical behaviour for compression stress states, it is necessary to avoid buckling effects. This requires the use of smaller specimens and, consequently, leads to supplementary difficulties in the acquisition and analysis of the experimental results, particularly for high strain values (maximum values of 1% [19] and 4% [18], depending on the test conditions). Therefore, it is important to evaluate the impact of taking also into account the strength differential (SD) effect, when using phenomenological models to describe the orthotropic behaviour of metallic materials that present a cubic structure, which are known to present a small SD effect.

In this context, the deep drawing of a cylindrical cup can help to evaluate the impact of the SD effect in the numerical prediction of the final shape. In fact, it was shown in previous works [6,20] that, as long as the stress component in the thickness direction is small, the outer flange will be submitted to a compression stress state. Therefore, the material behaviour will be dictated by the stress and r-values predicted for this stress state. In addition, both the compression yield stresses and the compression anisotropy coefficients in the RD will have a direct impact on the material behaviour at the transverse direction (TD) and *vice-versa*. In fact, the behaviour of the rim in the direction defined by θ with RD is controlled by the material compression properties in the direction defined by $90 - \theta$. Also, a lower value of the anisotropy coefficient leads to lower cup height, whereas lower values of the yield stresses lead to higher cup height [5]. Thus, the study of a cylindrical cup facilitates the analysis of the impact of both the compression yield stresses and r-values in-plane directionalities on the cup final shape.

Despite the previously mentioned difficulties in the experimental characterization of the mechanical behaviour of thin metallic sheets under compression stress states, it is important to analyse the impact of the SD effect on the final shape of deep drawn components. Therefore, this effect is taken into account in the finite element analysis by including a small tension-compression asymmetry in the yield stresses in-plane directionalities. In this context, it is also important to separate the influence of the SD effect from the orthotropic behaviour of the material. Thus, the type of data used to identify the anisotropy parameters of a yield criterion that neglects the SD effect is also analysed.

In this study, the DD3MAT (contraction of 'Deep Drawing 3D MATerials parameters identification') in-house code is used to identify the anisotropy parameters of a AA2090-T3 aluminium alloy, considering two yield criteria: (i) the Cazacu et al. [16],

which accounts for both tension-compression asymmetry and orthotropic plastic behaviour, considering one (CPB06) and two (CPB06ex2) linear transformations of the deviatoric stress tensor; and (ii) the Cazacu and Barlat [21] yield criterion. The later was selected due to its flexibility in describing highly anisotropy in-plane behaviour, associated with the high number of anisotropy parameters, although not allowing the description of the SD effect. In the following section, the yield criteria are briefly presented, as well as some other relevant details concerning the constitutive model adopted. In section 3, the strategy adopted for the anisotropy parameters identification procedure is described and applied to calibrate the yield criteria for the AA2090-T3. The details concerning the cylindrical cup forming process selected are given in section 4, which also presents and discusses the results obtained in the numerical simulation, particularly the earing profiles and the thickness distributions predicted. Finally, in the last section, the main conclusions are summarized.

2. Constitutive model

The Cazacu et al. [16] yield criterion allows the description of both the orthotropic behaviour and the SD effect, i.e. tension-compression asymmetry. The equivalent stress $\bar{\sigma}$ associated with the orthotropic form of the CPB06 yield criterion is defined as

$$\bar{\sigma} = B\left[\left(|s_1| - k\,s_1\right)^a + \left(|s_2| - k\,s_2\right)^a + \left(|s_3| - k\,s_3\right)^a\right]^{\frac{1}{a}} \tag{1}$$

where the exponent a is considered to be a positive integer, and k is a material parameter that allows defining the SD effect, when considering an isotropic material. However, has shown in [22], when anisotropy is taken into account different tension-compression ratios, σ^T/σ^C, can be obtained for the three orthotropic axis, i.e. the k parameter alone does not define the SD effect. s_1, s_2 and s_3 are the principal values of the tensor $\mathbf{s}$ resulting from the linear transformation proposed by Barlat et al. [23], such that $\mathbf{s} = \mathbf{C} : \boldsymbol{\sigma}'$. $\boldsymbol{\sigma}'$ is the deviatoric stress tensor and $\mathbf{C}$ is a constant 4$^\text{th}$-order transformation tensor. Adopting the Voigt notation, for 3-D stress conditions, the tensor $\mathbf{C}$ involves nine independent anisotropy coefficients and is expressed in the principal axis of anisotropy as

$$\mathbf{C} = \begin{bmatrix} C_{11} & C_{12} & C_{13} & 0 & 0 & 0 \\ C_{12} & C_{22} & C_{23} & 0 & 0 & 0 \\ C_{13} & C_{23} & C_{33} & 0 & 0 & 0 \\ 0 & 0 & 0 & C_{44} & 0 & 0 \\ 0 & 0 & 0 & 0 & C_{55} & 0 \\ 0 & 0 & 0 & 0 & 0 & C_{66} \end{bmatrix}, \tag{2}$$

B is a constant defined such that $\bar{\sigma}$ reduces to the tensile yield stress in RD,

$$B = \left[\frac{1}{\left(|\phi_1| - k\,\phi_1\right)^a + \left(|\phi_2| - k\,\phi_2\right)^a + \left(|\phi_3| - k\,\phi_3\right)^a}\right]^{\frac{1}{a}} \tag{3}$$

with

$$\begin{Bmatrix} \phi_1 \\ \phi_2 \\ \phi_3 \end{Bmatrix} = \begin{Bmatrix} (2/3)C_{11} - (1/3)C_{12} - (1/3)C_{13} \\ (2/3)C_{21} - (1/3)C_{22} - (1/3)C_{23} \\ (2/3)C_{31} - (1/3)C_{32} - (1/3)C_{33} \end{Bmatrix} \tag{4}$$

The convexity of the yield criterion is guaranteed for any integer $a \geq 2$ and $k \in [-1, 1]$ [16]. Note that, for yield criteria based on the linear transformation of the deviatoric stress tensor, the number of transformations is unlimited, in terms of formulation, with the only constrain being the number of experimental data available. Therefore, since nine anisotropy parameters may not be sufficient for describing the behaviour of materials showing pronounced in-plane anisotropy, Plunkett et al. [24] extended the CPB06 yield criterion to consider two linear transformations (CPB06ex2), thus doubling the number of anisotropy coefficients from 9 to 18. For the CPB06ex2, the equivalent stress $\bar{\sigma}$ associated with its orthotropic form is defined as

$$\bar{\sigma} = B \left[\begin{array}{c} (\,|s_1| - k\,s_1)^a + (\,|s_2| - k\,s_2)^a + (\,|s_3| - k\,s_3)^a \\ +(\,|s'_1| - k'\,s'_1)^a + (\,|s'_2| - k'\,s'_2)^a + (\,|s'_3| - k'\,s'_3)^a \end{array} \right]^{\frac{1}{a}} \tag{5}$$

B remains a constant defined such that $\bar{\sigma}$ reduces to the tensile yield stress in RD,

$$B = \left[\cfrac{1}{\begin{array}{c} (\,|\phi_1| - k\,\phi_1)^a + (\,|\phi_2| - k\,\phi_2)^a + (\,|\phi_3| - k\,\phi_3)^a \\ +(\,|\phi'_1| - k'\,\phi'_1)^a + (\,|\phi'_2| - k'\,\phi'_2)^a + (\,|\phi'_3| - k'\,\phi'_3)^a \end{array}} \right]^{\frac{1}{a}}, \tag{6}$$

with the same definition for the ϕ_i, $i = 1, 2, 3$ as in Eq. (4) and

$$\begin{Bmatrix} \phi'_1 \\ \phi'_2 \\ \phi'_3 \end{Bmatrix} = \begin{Bmatrix} (2/3)C'_{11} - (1/3)C'_{12} - (1/3)C'_{13} \\ (2/3)C'_{21} - (1/3)C'_{22} - (1/3)C'_{23} \\ (2/3)C'_{31} - (1/3)C'_{32} - (1/3)C'_{33} \end{Bmatrix} \tag{7}$$

The convexity is still guaranteed for any integer $a \geq 2$, $k \in [-1, 1]$ and $k' \in [-1, 1]$ since the use of one or several linear transformations does not affect convexity of the yield function [25,26]. For $\mathbf{C} = \mathbf{C}'$ and $k = k'$, the CPB06ex2 yield criterion reduces to the CPB06, i.e. considering only one linear transformation. Moreover, the CPB06 reduces to the von Mises yield criterion when $a = 2$, $k = 0$, $C_{ii} = 1.0$, with $i = 1, ..., 6$ and $C_{ij} = 0.0$, with $i, j = 1, ..., 3$.

The CB2001 [21] yield criterion is a generalization of the Drucker's isotropic criterion to orthotropy and, in its general form, is given by

$$\bar{\sigma} = \left\{ 27 \left[(J_2^0)^3 - c(J_3^0)^2 \right] \right\}^{\frac{1}{6}} \tag{8}$$

where J_2^0 and J_3^0 are the second and third generalized invariants of the effective stress tensor $\mathbf{\Sigma}$, defined as

$$\begin{aligned} J_2^0 = &\frac{a_1}{6}(\Sigma_{11} - \Sigma_{22})^2 + \frac{a_2}{6}(\Sigma_{11} - \Sigma_{33})^2 + \frac{a_3}{6}(\Sigma_{11} - \Sigma_{33})^2 \\ &+ a_4 \Sigma_{12}^2 + a_5 \Sigma_{13}^2 + a_6 \Sigma_{23}^2 \end{aligned} \tag{9}$$

$$\begin{aligned}
J_3^0 &= (1/27)(b_1 + b_2)\Sigma_{11}^3 + (1/27)(b_3 + b_4)\Sigma_{22}^3 \\
&+ (1/27)[2(b_1 + b_4) - b_2 - b_3]\Sigma_{33}^3 \\
&- (1/9)(b_1\Sigma_{22} + b_2\Sigma_{33})\Sigma_{11}^2 - (1/9)(b_3\Sigma_{33} + b_4\Sigma_{11})\Sigma_{22}^2 \\
&- (1/9)[(b_1 - b_2 + b_4)\Sigma_{11} + (b_1 - b_3 + b_4)\Sigma_{22}]\Sigma_{33}^2 \\
&+ (2/9)(b_1 + b_4)\Sigma_{11}\Sigma_{22}\Sigma_{33} \\
&- (\Sigma_{13}^2/3)[2b_9\Sigma_{22} - b_8\Sigma_{33} - (2b_9 - b_8)\Sigma_{11}] \\
&- (\Sigma_{12}^2/3)[2b_{10}\Sigma_{33} - b_5\Sigma_{22} - (2b_{10} - b_5)\Sigma_{11}] \\
&- (\Sigma_{23}^2/3)[(b_6 - b_7)\Sigma_{11} - b_6\Sigma_{22} - b_7\Sigma_{33}] + 2b_{11}\Sigma_{12}\Sigma_{23}\Sigma_{13}
\end{aligned} \tag{10}$$

where c, $a_1, ..., a_6$ and $b_1, ..., b_{11}$ are the anisotropy parameters. Σ_{ij}, $i, j = 1, 2, 3$ are the effective stress components defined in the material frame. The conditions that guarantee the convexity of CB2001 are unknown, excepted when assuming in-plane isotropic behaviour, for which $c \in [-3.75, 2.25]$ [21].

The yield condition is defined as

$$F(\bar{\sigma}, Y) = \bar{\sigma} - Y = 0 \tag{11}$$

where Y is the flow stress, which depends of the hardening law selected, such that the yield stress is Y_0.

The constitutive model adopted considers an associated flow rule, meaning that the yield function serves as the plastic potential for determining the plastic strain increment. The plastic strain rate tensor, $\mathbf{D}^p$, is determined according to

$$\mathbf{D}^p = \dot{\lambda}\frac{\partial F(\bar{\sigma}, Y)}{\partial \boldsymbol{\sigma}} \tag{12}$$

The equivalent stress is given by Eq. (1), (5) or (8), depending on the yield criterion adopted. $\dot{\lambda}$ is a scalar value designated by plastic multiplier that can be demonstrated to be equal to the equivalent plastic strain rate, $\dot{\bar{\varepsilon}}^p$. The equivalent plastic strain is defined as

$$\bar{\varepsilon}^p = \int_0^t \dot{\bar{\varepsilon}}^p dt = \int_0^t \frac{\boldsymbol{\sigma}'}{\bar{\sigma}} : \mathbf{D}^p dt. \tag{13}$$

For further details concerning the constitutive model and its implementation, please refer to [20,27].

3. Material parameters identification

The anisotropy parameters should be determined such that the yield criterion reproduces the material's mechanical behaviour as close as possible. When adopting a classical identification strategy, the usual experimental results used for the identification of the anisotropy parameters are the yield stresses and the r-values obtained from in-plane tension for different angles (θ) with RD. These tests are commonly performed for several directions in the sheets plane, and can be complemented with other trajectories, like the biaxial yield stress, σ_b, and the biaxial anisotropy coefficient r_b

[28,29]. In case of yield criteria capable of describing SD effects, uniaxial compression experimental results are also necessary.

The DD3MAT in–house code [30] serves for determining yield criteria parameters that accurately adjust a given material's experimental behaviour. The procedure adopted is based on the minimization of an error function that evaluates the difference between estimated and experimental values,

$$
\begin{aligned}
F(\mathbf{A}) = {} & w_{\sigma_\theta^{\mathrm{T}}} \sum_{\theta=0}^{90} \left(\sigma_\theta^{\mathrm{T}}(\mathbf{A}, \bar{\varepsilon}^{\mathrm{p}}) \big/ \sigma_\theta^{\mathrm{T}}(\bar{\varepsilon}^{\mathrm{p}}) - 1 \right)^2 + w_{\sigma_\theta^{\mathrm{C}}} \sum_{\theta=0}^{90} \left(\sigma_\theta^{\mathrm{C}}(\mathbf{A}, \bar{\varepsilon}^{\mathrm{p}}) \big/ \sigma_\theta^{\mathrm{C}}(\bar{\varepsilon}^{\mathrm{p}}) - 1 \right)^2 \\
& + w_{r_\theta^{\mathrm{T}}} \sum_{\theta=0}^{90} \left(r_\theta^{\mathrm{T}}(\mathbf{A}) \big/ r_\theta^{\mathrm{T}} - 1 \right)^2 + w_{\sigma_{\mathrm{b}}} \left(\sigma_{\mathrm{b}}(\mathbf{A}, \bar{\varepsilon}^{\mathrm{p}}) \big/ \sigma_{\mathrm{b}}(\bar{\varepsilon}^{\mathrm{p}}) - 1 \right)^2 \\
& + w_{r_{\mathrm{b}}} \left(r_{\mathrm{b}}(\mathbf{A}) \big/ r_{\mathrm{b}} - 1 \right)^2,
\end{aligned}
\tag{14}
$$

with $\mathbf{A}$ representing the set of parameters of the respective yield criterion. $\sigma_\theta^{\mathrm{T}}(\bar{\varepsilon}^{\mathrm{p}})$, $\sigma_\theta^{\mathrm{C}}(\bar{\varepsilon}^{\mathrm{p}})$ and r_θ are the experimental yield stresses in tension, compression, and anisotropy coefficients determined in uniaxial tension, respectively. These are obtained from the uniaxial tests for a specific orientation (θ) with respect to RD. σ_{b} is the experimental yield stress obtained from the equibiaxial tensile test and r_{b} is the experimental anisotropy coefficient obtained from the disc compression test. $\sigma_\theta^{\mathrm{T}}(\mathbf{A}, \bar{\varepsilon}^{\mathrm{p}})$, $\sigma_\theta^{\mathrm{C}}(\mathbf{A}, \bar{\varepsilon}^{\mathrm{p}})$, $r_\theta^{\mathrm{T}}(\mathbf{A})$, $\sigma_{\mathrm{b}}(\mathbf{A}, \bar{\varepsilon}^{\mathrm{p}})$ and $r_{\mathrm{b}}(\mathbf{A})$ are the correspondent values predicted from the adopted yield criterion. Such procedure can be considered a generalization of the one proposed by Banabic et al. [31], where the weighting factors, $w_{\sigma_\theta^{\mathrm{T}}}$, $w_{\sigma_\theta^{\mathrm{C}}}$, w_{r_θ}, $w_{\sigma_{\mathrm{b}}}$ and $w_{r_{\mathrm{b}}}$, are used to balance the influence of the experimental data. The selection of the weighting factors is a manual procedure strongly dependent on the users' expertise and knowledge.

When considering thin metallic sheets, the off-plane properties are difficult to obtain. For the particular case of the CPB06, the yield criterion presents 9 anisotropy parameters and the k value. However, since the anisotropy parameters, C_{44} and C_{55}, cannot be evaluated, the corresponding isotropic values are usually adopted, i.e. 1.0. Moreover, the C_{11} parameter is also considered equal to 1.0 to avoid equivalent sets of parameters, as discussed in [27]. Thus, a total of 6 anisotropy parameters and the k value must be identified. As for the case of the CPB06ex2, the same premises are considered. In this case, $C_{44}' = C_{55}' = 1.0$ as well as $C_{11}' = 1.0$, totalling 12 anisotropy parameters and the k and k' values to be identified. For the CB2001 yield criterion, a_5, a_6 and b_k ($k = 6, 7, 8, 9, 11$) are the ones corresponding to the off-plane properties that cannot be evaluated and are assumed as equal to the isotropic values, i.e. 1.0. Therefore, in this case, it is necessary to identify a total of 10 anisotropy parameters and the c value.

The identification procedure assumes that $k \in [-1, 1]$, $k' \in [-1, 1]$, $C_{ij} \in [-4, 6]$ and $C_{ij}' \in [-4, 6]$ for $i = j$, and $C_{ij} \in [-5, 5]$ and $C_{ij}' \in [-5, 5]$ for the remaining parameters, in order to allow the same interval around the isotropic values. The identification procedure is repeated for each integer value $a \in [2, 12]$, in order to select the one that renders the best fit, which is evaluated based on the comparison of the objective function (see Eq. (14)), but also on the in-plane evolutions of both stresses and r-values, for tension and compression. Note that, since the compression r-values are not considered in the objective function, because they are not available from the experimental

data, the values predicted may have strange evolutions or even no physical meaning (e.g. $r < 0$). Thus, their in-plane evolution must also be carefully monitored and taken into account when selecting the a value. For the CB2001, it is assumed that $a_i \in [-10, 10]$, $b_i \in [-10, 10]$ and $c \in [-3.75, 2.25]$. The minimization process adopted for this yield criterion includes testing the convexity of the yield surface, for several planes in the stress space [20].

The optimization algorithm adopted in DD3MAT is based on a downhill-simplex derivative-free method, allowing to find the minimum of the objective function in a multidimensional space, with a low computational cost.

3.1. Application to AA2090-T3 aluminium alloy

The CPB06, CPB06ex2 and CB2001 yield criteria parameters identification are performed for an AA2090-T3 aluminium alloy since uniaxial tension, uniaxial compression and equibiaxial experimental results are available from the literature [13]. The available data is presented in Table 1, which considers experimental uniaxial tension yield stresses and anisotropy coefficients, and uniaxial compression yield stresses, for different orientations with the rolling direction. The experimental yield stress and r-value obtained from the balanced biaxial test and disk compression test are also included. Therefore, a total of 23 experimental values are known, which reduce to 16 if the data corresponding to the compression tests is neglected. Therefore, the number of anisotropy parameters is lower than the number of experimental values, i.e. the optimization problem, defined by the objective function presented in Eq. (14), is always over-constrained.

The CPB06 and CPB06ex2 versions of the yield criterion are used to simultaneously describe the material mechanical behaviour in tension and compression. Note that the CPB06 formulation guarantees that the yield stress, Y_0, considered is always equal to the one obtained for the uniaxial tensile test performed along RD, σ_{RD}^T (see Eq. (1) and Eq. (5)). Therefore, previous results indicate that the value considered for the yield stress, Y_0, defined by the hardening law, should be in accordance with σ_{RD}^T to enable an accurate description of the in-plane yield stresses directionalities [22].

Two sets of anisotropy parameters are identified for the CB2001, considering all the experimental results, except that: one uses the tension yield stresses (CB2001-T) and the other the compression ones (CB2001-C). In fact, since this yield criterion does not

Table 1. Experimental uniaxial tension and compression yield stresses, r-values and stress ratios, for the AA2090-T3 [14].

Test direction [º]	r-value	$\sigma_\theta^{Y_T}$ [MPa]	$\sigma_\theta^{Y_C}$ [MPa]	Stress ratio $\sigma_\theta^{Y_T}/\sigma_\theta^{Y_C}$
0º	0.210	279.62	248.02	1.127
15º	0.330	269.72	260.75	1.034
30º	0.690	255.00	255.00	1.000
45º	1.580	226.77	237.75	0.954
60º	1.050	227.50	245.75	0.926
75º	0.550	247.20	263.75	0.937
90º	0.690	254.45	266.48	0.955
σ_b		289.40		
r_b	0.670			

allow the description of the SD effect, it was decided to use its flexible behaviour to isolate the influence of the material behaviour in compression, in order to be evidenced in the numerical example.

The weighting coefficients considered for both CPB06 and CPB06ex2 are the same: $w_{r_\theta} = 0.1$ for $\theta \in [0, 90]$ except $w_{r_{45}} = 0.25$, in order to capture the higher r-value at 45°. For the yield stresses in tension, the weighting coefficients are considered unitary for all directions, i.e. $w_{\sigma_\theta^T} = 1.0$ for $\theta \in [0, 90]$. The yield stresses in compression consider the weighting coefficients as $w_{\sigma_\theta^C} = 1.1$ for $\theta \in [0, 90]$. Both biaxial values consider unitary weights as $w_{r_b} = 1.0$ and $w_{\sigma_b} = 1.0$. This set of weighting coefficients was tested for each integer value $a \in [2, 12]$, leading to the selection of the following exponents: $a = 3$ for CPB06 and $a = 5$ for CPB06ex2.

The weighting coefficients considered for the CB2001 identifications differ, since different features must be captured when considering tension or compression yield stress evolutions. For the CB2001-T, $w_{r_\theta} = 0.1$ for $\theta \in [0, 90]$ except $w_{r_{45}} = w_{r_{75}} = w_{r_{90}} = 0.5$, $w_{\sigma_0^T} = 2.0$, $w_{\sigma_\theta^T} = 0.1$ for $\theta \in [15, 45]$ and $w_{\sigma_\theta^T} = 1.0$ for $\theta \in [60, 90]$. For the biaxial values, $w_{r_b} = 0.1$ and $w_{\sigma_b} = 0.5$. For the CB2001-C, $w_{r_\theta} = 0.1$ for $\theta \in [0, 90]$ except $w_{r_{45}} = w_{r_{75}} = w_{r_{90}} = 0.2$, $w_{\sigma_\theta^T} = 2.0$ for $\theta \in [0, 30]$ and $w_{\sigma_\theta^T} = 1.0$ for $\theta \in [45, 90]$. Note that the uniaxial tension yield stress were assumed equal to the compressive ones, since the CB2001 does not take into account the SD effect. For the biaxial values, $w_{r_b} = 0.1$ and $w_{\sigma_b} = 1.0$, for both cases

Figure 1 presents the comparison between the experimental and predicted r-values and yield stresses for the yield criteria. Although there is no experimental data available concerning the r-values in compression, the predicted values are also presented to allow the analysis of their impact in the numerical simulation results. Also note that, since the CB2001 does not allow the description of the SD effect, the same in-plane evolution is predicted for both tension and compression stress states. Regarding the r-values, the CPB06 can only describe the global experimental trend with accurate values for the RD and TD and a maximum for about 45°. The behaviour in tension and compression is similar. When using the CPB06ex2, an improvement is verified, with all the experimental values well approximated. The difference in behaviour between tension and compression becomes
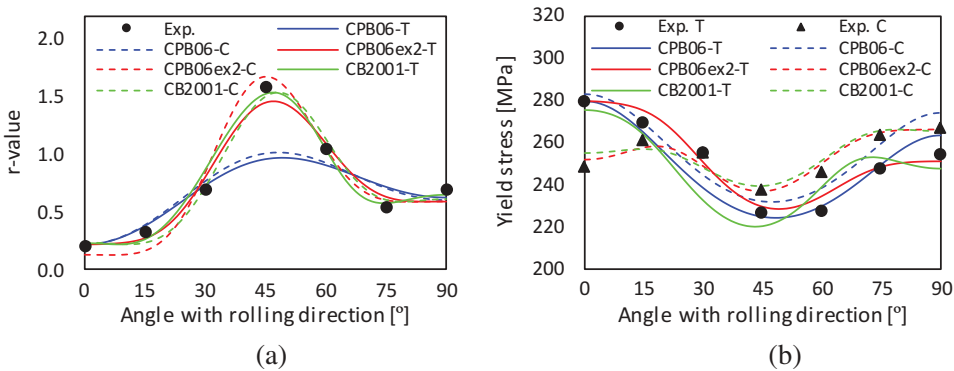

Figure 1. Experimental and predicted: (a) r-values and (b) yield stresses for the AA2090-T3 considering the best fit for the CPB06, CPB06ex2 and CB2001.

more pronounced, mainly for 45º. A very good prediction is also obtained by both CB2001 identifications which, accordingly, present an in-plane evolution of the r-value in tension similar to the one predicted for the CPB06ex2. As for the yield stresses evolution, while CPB06 is able to describe both tension and compression, the 6 available anisotropy parameters are not enough to enable the description of this material's anisotropic behaviour. The yield stresses in tension are well described. However, while the yield stresses in compression are well described for angles higher than 30º, it fails to describe the inflection point which would allow an accurate fit for $\theta \in [0, 30]$. The CPB06ex2, however, is able to accurately describe both the yield stresses in tension and compression, including the inflection points. The CB2001 accurately describes either the yield stresses in tension or compression, depending on which were used in the identification procedure, with an evolution very close to the one presented by the CPB06ex2, particularly for the compression yield stresses.

Regarding the biaxial values, Table 2 presents the comparison between the experimental and the numerical prediction. For the σ_b, the CPB06 shows the worst prediction, underpredicting the experimental value. Both the CPB06ex2 and CB2001 yield criteria predict values very close to the experimental ones. The r_b is well predicted by all the criteria, with the CPB06ex2 presenting the closest value to the experimental one. Thus, when comparing the yield surfaces in the σ_{11}, σ_{22} plane (with $\sigma_{33} = 0$), as shown in Figure 2, it is possible to confirm the similarities between the ones predicted by the CPB06ex2 and the CB2001, since both yield criteria present a similar number of anisotropy parameters. When considering the two CB2001 identifications, it is possible to confirm a slight change of shape, induced by the different in-plane trends. Moreover, it should be mentioned that the AA2090-T3 presents a small SD effect, as can be seen in Table 1, by the analysis of the stress ratios. As shown in Table 2, the CPB06ex2 yield criterion is the only one that accurately captures the stress ratios, for both 0 and 90º to the rolling direction. Finally, the anisotropy parameters obtained for the considered yield criteria are presented in Table 3.

4. Numerical simulation

The numerical simulation of a cylindrical cup drawing was performed in order to analyse the influence of considering different behaviours for both the yield stresses and the r-values in tension and compression in the final shape. The selected example is based on the work of Yoon et al. [19]. All numerical simulations were performed with the static implicit in-house solver DD3IMP (contraction of 'Deep Drawing 3-D IMPlicit'), specifically developed to simulate sheet metal forming processes [32] and continuously updated to enable an improved description of the contact conditions [33,34] and computational efficiency [35].

Table 2. Experimental and numerically predicted biaxial values and stress ratios for the AA2090-T3.

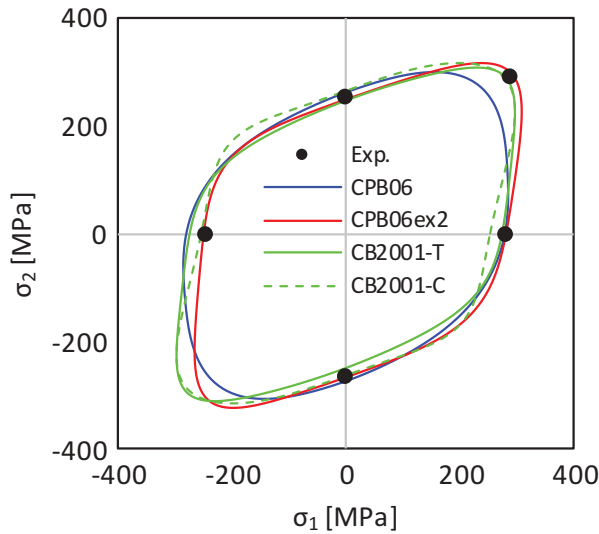|	σ_b	r_b	Stress ratio $\sigma_0^{Y_T}/\sigma_0^{Y_C}$	Stress ratio $\sigma_{90}^{Y_T}/\sigma_{90}^{Y_C}$
Experimental	289.40	0.670	1.127	0.955
CPB06	253.58	0.657	0.989	0.962
CPB06ex2	293.07	0.671	1.111	0.943
CB2001-T	285.89	0.660	1.000	1.000
CB2001-C	283.83	0.696	1.000	1.000

Figure 2. Predicted yield surfaces in the σ_{11}, σ_{22} plane (with $\sigma_{33} = 0$) for the AA2090-T3 considering the best fit for the CPB06, CPB06ex2 and CB2001.

Table 3. Identified parameters for the AA2090-T3 for the considered yield criteria ($C_{11} = C_{44} = C_{55} = C'_{11} = C'_{44} = C'_{55} = 1.0$, and a_5, a_6 and b_k ($k = 6, 7, 8, 9, 11$) $= 1.0$).

CPB06	C_{22}	C_{33}	C_{66}	C_{23}	C_{13}	C_{12}	k
	1.357	0.998	−1.283	0.105	−0.196	0.242	−0.020
CPB06ex2	C_{22}	C_{33}	C_{66}	C_{23}	C_{13}	C_{12}	k
	0.739	−0.435	1.775	0.362	1.285	0.740	0.252
	C'_{22}	C'_{33}	C'_{66}	C'_{23}	C'_{13}	C'_{12}	k'
	1.437	−1.888	−1.526	−0.463	−0.939	−0.223	−0.029
CB2001-T	a_1	a_2	a_3	a_4			c
	1.358	1.848	1.075	1.709			0.857
	b_1	b_2	b_3	b_4	b_5		b_{10}
	5.357	−0.623	−4.386	−3.654	−6.046		−0.882
CB2001-C	a_1	a_2	a_3	a_4			c
	1.803	0.975	1.209	1.461			1.888
	b_1	b_2	b_3	b_4	b_5		b_{10}
	−5.000	0.130	0.277	4.027	2.807		−0.200

4.1. Problem description

The schematics of the cup drawing process and main dimensions are shown in Figure 3 (a). The blank sheet is circular in shape with a diameter of 158.76 mm and a thickness of 1.6 mm. The blank-holder force has a value of 22.2 kN, corresponding to the minimum value predicted to avoid wrinkles [19]. The contact with friction conditions is described by the Coulomb's law, using a constant friction coefficient, μ, of 0.1.

Due to geometrical and material symmetries, only a quarter of the global structure is modelled. The sheet is discretized with 8-node hexahedral finite elements, combined with a selective-reduced integration technique [36]. Figure 3(b) shows the in-plane sheet discretization used, considering both a structured and an unstructured zone to facilitate the construction of a regular mesh. The model considers two layers of elements in the thickness direction, leading to a total number of 19,648 elements.
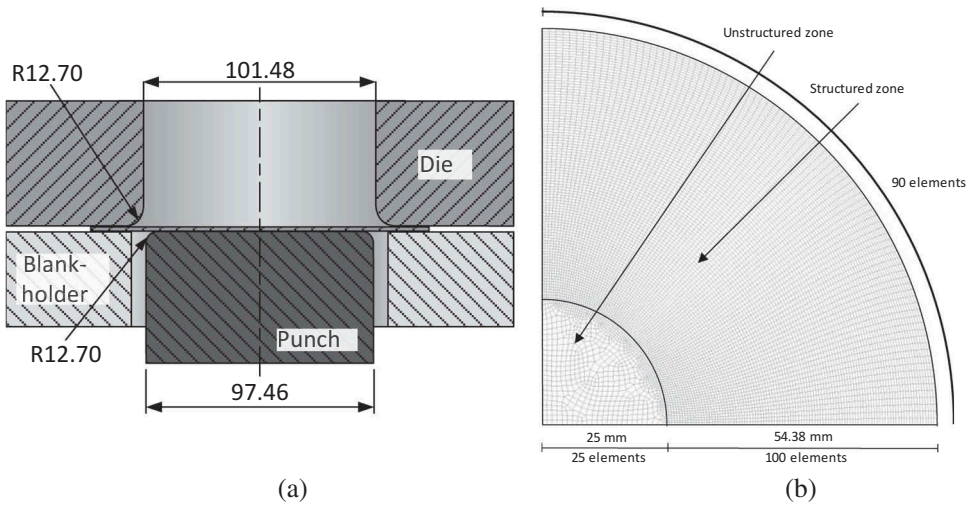
Figure 3. (a) Schematic of the cup drawing and main dimension and (b) in-plane blank sheet discretization.

The material's mechanical behaviour is assumed to be isotropic in the elastic regime, being described by the Young's modulus, E, and the Poisson ratio, v. The plastic behaviour is described using an isotropic work hardening Swift type law, given by

$$Y(\bar{\varepsilon}^{p}) = K(\varepsilon_0 + \bar{\varepsilon}^{p})^{n}, \tag{15}$$

where Y is the flow stress and $\bar{\varepsilon}^{p}$ is the equivalent plastic strain. The elastic properties and the material parameters of the hardening law used in the numerical model are presented in Table 4.

4.2. Results and discussion

The comparison between the experimental and the numerically predicted cup height *vs.* angle from RD of the final cup, as well as the predicted thickness strains, are presented in Figure 4. Regarding the earing profile, the CPB06 predicts only one ear with a maximum at around 45º, whereas the experimental one is around 50º. Also, it is not able to predict the baseline for $\theta \in [0°, 25°]$. The CPB06ex2 and the CB2001-C present very similar predictions, capturing the baseline for $\theta \in [0°, 25°]$. This can be related with the similarities presented in the in-plane distribution of the compression *r*-value for $\theta \in [65°, 90°]$, since the in-plane evolution of the compression yield stress is also quite similar (see Figure 1). The CB2001-T for $\theta \in [0°, 25°]$ presents a small ear as a result of the trend predicted for the tensile yield stresses $\theta \in [60°, 90°]$. The CPB06ex2 maximum is closer to the experimental one, not only in terms of value but also location, with also a closer prediction for $\theta \in [45°, 90°]$. In fact, for $\theta \in [45°, 90°]$, both CPB06ex2 and CB2001-C present the same trend, although the CB2001-C presents a slightly lower height. The fact that the CPB06ex2 predicts an higher height close to 45º can also be related with the higher value of the compression *r*-value (see Figure 1(a)), compared with the one predicted by CB2001-C, which is known to lead to a higher cup height. However, based on the slightly lower value of the compression *r*-value for $\theta \in [0°, 30°]$, predicted

Table 4. Elastic properties and material parameters of the work hardening law.

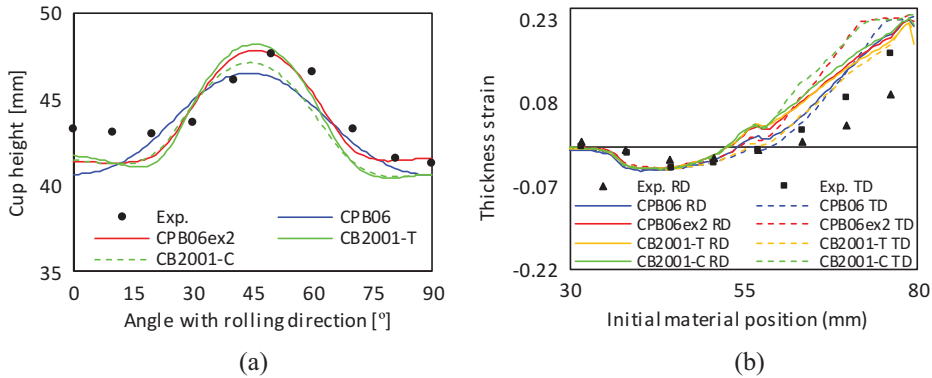| Elastic properties	Isotropic hardening (Swift law)
$E = 74$ [GPa]	$K = 646$ [MPa]
$v = 0.34$	$\varepsilon_0 = 0.025$
	$n = 0.227$
	$Y_0 = 279.62$ [MPa]

(a)　　　　　　　　　　(b)

Figure 4. Comparison between experimental and numerically predicted: (a) cup height *vs.* angle from RD and (b) thickness strain.

by the CPB06ex2 when compared with the CB2001-C, one would expect a lower high of the cup. In this context, it should be mentioned that lower values of the yield stresses lead to higher cup height [5,20]. This also explains why the CB2001-T presents the highest amplitude for the ears, dictated by the higher amplitude predicted to the in-plane distribution of the tensile yield stresses. Finally, it should be mentioned that slight changes in the blank-holder force distribution, resulting from the orthotropic behaviour, disable a direct evaluation of the cup height from the in-plane directionalities [20].

Regarding the thickness strain distribution, all yield criteria predict a trend close to the experimental one, even though the thickness strain is globally overpredicted in the cup wall, for both directions. The fact that the thickening is overestimated, whatever the yield criterion adopted, can be related to the lower average height estimated for the cup. Globally, the CPB06 and, particularly, the CB2001-T cannot accurately predict the difference between the thickness strains along the RD and the TD directions. For the CPB06, the yield stress predicted for the TD is only slightly lower than for the RD direction, resulting in the similar trend. However, the CB2001-T presents a value for the yield stress predicted for the TD clearly lower than the one for RD, which results in a trend opposite to the experimental one. As for the CPB06ex2 and CB2001-C, both yield criteria predict higher thickening in the cup wall for the TD direction. This is a consequence of the compression yield stresses predicted since, for both the CPB06ex2 and the CB2001-C, the compression yield stresses for RD are lower than the ones predicted for the TD. As previously mentioned, the value selected for the blank-holder force corresponds to the minimum value predicted to avoid wrinkles. However, due to the strong orthotropic behaviour of the material, the blank-holder force is not evenly distributed in the flange. Moreover, since the tool presents no blank-holder stopper a slight squeeze occurs before the

blank loses contact with this tool, particularly for the material located closer to the RD (see Figure 4 (b)), where there are also higher differences between the experimental and the numerical results. In fact, these factors make the numerical prediction more sensitive to the contact with friction conditions [20].

5. Conclusion

In this paper, the anisotropy parameters for the CPB06, CPB06ex2 and CB2001 yield criteria were identified, following a classical strategy, for an AA2090-T3 aluminium alloy. The identification results show that the CPB06 is able to describe the tension-compression asymmetry, but it is not flexible enough for describing materials that present pronounced orthotropic behaviour. Considering two linear transformations of the deviatoric stress tensor, CPB06ex2, enables the doubling of the number of anisotropy parameters, leading to an accurate description of yield stresses and r-values in-plane directionalities, for both tension and compression states. However, particular care was taken in the identification procedure, concerning the in-plane compression r-values, since when this experimental data is unavailable, the predictions can lead to strange distributions.

The CB2001 yield criterion was considered to evaluate the impact of taking into account the SD effect in the numerical predictions of the earing profile of a cylindrical cup. This yield criterion is known for its flexibility, presenting a number of anisotropy parameters similar to the CPB06ex2. However, due to its inability to describe the SD effect, two different sets of experimental data were adopted in the anisotropy parameters identification procedure. The first considers the yield stresses evaluated from the uniaxial tensile tests and the second set from compression tests. Both identifications lead to a proper description of the in-plane r-values and yield stresses evolutions (i.e. the ones considered in the identification procedure). Thus, the results obtained with the CB2001 are similar to the ones of the CPB06ex2 in terms of cup height.

Concerning the cylindrical cup forming operation, the earing profile of the cup and the thickness strain distribution along RD and TD are the main parameters analysed. The comparison of the experimental and numerical results show that, for this example, for which the earing profile and the cup height is driven mainly by the description of the compressive stress states, considering the compression yield stresses are critical to obtain accurate predictions. In fact, the compression yield stresses directionalities seem to play a major role when it comes to the thickness predictions. Thus, a good prediction of the material in-plane directionalities, including the compression yield stresses, is important for the numerical simulation of deep drawing processes, even for materials presenting small tension-compression asymmetry.

Disclosure statement

No potential conflict of interest was reported by the authors.

Funding

ORCID

P.D. Barros ⬤ http://orcid.org/0000-0001-7098-404X
M.C. Oliveira ⬤ http://orcid.org/0000-0001-8032-7262
J.L. Alves ⬤ http://orcid.org/0000-0001-8714-4880
L.F. Menezes ⬤ http://orcid.org/0000-0002-4703-9346

References

[1] Banabic D. Sheet metal forming processes. Berlin Heidelberg: Springer. Springer-Verlag; 2010.
[2] Tresca H-É. Mémoire sur l'écoulement des corps solides soumis à de fortes pressions. Comptes Rendus l'Académie Des Sci Paris. 1864;59:754–758.
[3] von Mises R Mechanik der festen korper im plastic-deformablen zustand. Nachrichten vos der K. gellesschaft des winssenschaften zu Gottingen. 1913;582–592.
[4] Hill RA. Theory of the yielding and plastic flow of anisotropic metals. Proc R Soc A Math Phys Eng Sci. 1948;193:281–297.
[5] Yoon JW, Dick RE, Barlat F. A new analytical theory for earing generated from anisotropic plasticity. Int J Plast. 2011;27:1165–1184.
[6] Barros PD, Alves JL, Oliveira M, et al. Tension-compression asymmetry modelling : strategies for anisotropy parameters identification. NUMIFORM 2016 12th International Conference Numerical. Methods Industrial Forming Processing. Troyes, France.MATEC Web Conf. 80 05002 (2016).
[7] Zidane I, Guines D, Léotoing L, et al. Development of an in-plane biaxial test for forming limit curve (FLC) characterization of metallic sheets. Meas Sci Technol. 2010;21:55701.
[8] Güner A, Soyarslan C, Brosius A, et al. Characterization of anisotropy of sheet metals employing inhomogeneous strain fields for Yld2000-2D yield function. Int J Solids Struct. 2012;49:3517–3527.
[9] Cooreman S, Lecompte D, Sol H, et al. Identification of mechanical material behavior through inverse modeling and DIC. Exp Mech. 2008;48:421–433.
[10] Prates PA, Oliveira MC, Fernandes JV. Identification of material parameters for thin sheets from single biaxial tensile test using a sequential inverse identification strategy. Int J Mater Form. 2016; 9(4): 547–571.
[11] Pottier T, Vacher P, Toussaint F, et al. Out-of-plane testing procedure for inverse identification purpose: application in sheet metal plasticity. Exp Mech. 2012;52:951–963.
[12] Zhang K, Holmedal B, Hopperstad OS, et al. Multi-level modelling of mechanical anisotropy of commercial pure aluminium plate: crystal plasticity models, advanced yield functions and parameter identification. Int J Plast. 2015;66:3–30.
[13] Barlat F, Lege DJ, Brem JC, et al. Constitutive behavior for anisotropic materials and application to a 2090 Al±Li alloy. In: Lowe T, Rollett A, Follansbee P, et al., editors. TMS annual meeting. New Orleans, LA: TMS; 1991. 189–203.
[14] Cazacu O, Barlat F. A criterion for description of anisotropy and yield differential effects in pressure-insensitive metals. Int J Plast. 2004;20:2027–2045.

[15] Drucker DC. Relation of experiments to mathematical theories of plasticity, journal of applied mechanics. ASME. 1949;16:A349–A357.

[16] Cazacu O, Plunkett B, Barlat F. Orthotropic yield criterion for hexagonal closed packed metals. Int J Plast. 2006;22:1171–1194.

[17] Plunkett B, Lebensohn RA, Cazacu O, et al. Anisotropic yield function of hexagonal materials taking into account texture development and anisotropic hardening. Acta Mater. 2006;54:4159–4169.

[18] Tritschler M, Butz A, Helm D, et al. Experimental analysis and modeling of the anisotropic response of titanium alloy Ti-X for quasi-static loading at room temperature. Int J Mater Form. 2014;7:259–273.

[19] Yoon JW, Barlat F, Chung K, et al. Earing predictions based on asymmetric nonquadratic yield function. Int J Plast. 2000;16:1075–1104.

[20] Barros PD, Neto DM, Alves JL, et al. DD3IMP, 3D fully implicit finite element solver : implementation of CB2001 yield criterion. Rom J Tech Sci - Appl Mech. 2015;60:105–136.

[21] Cazacu O, Barlat F. Generalization of drucker's yield criterion to orthotropy. Math Mech Solids. 2001;6:613–630.

[22] Barros PD, Oliveira MC, Alves JL. Modelling of tension-compression asymmetry and orthotropic anisotropy in case of thin metallic sheets: identification procedure and case studies. In: Hora P, et al. editor, Zurich: Institute of Virtual Manufacturing, ETH Zurich; 2015. p. 149–154. https://www.ethz.ch/content/dam/ethz/special-interest/mavt/virtual-manufacturing/ivp-dam/News_Events/ftf2015/FTF2015_Proceedings_Digital_2015-08-12.pdf

[23] Barlat F, Maeda Y, Chung K, et al. Yield function development for aluminum alloy sheets. J Mech Phys Solids. 1997;45:1727–1763.

[24] Plunkett B, Cazacu O, Barlat F. Orthotropic yield criteria for description of the anisotropy in tension and compression of sheet metals. Int J Plast. 2008;24:847–866.

[25] Eggleston. General properties of convex functions. Convexity. 1958.

[26] Rockafellar. Convex functions. Convex anal. 1972.

[27] Barros PD, Alves JL, Oliveira MC, et al. Modeling of tension-compression asymmetry and orthotropy on metallic materials: numerical implementation and validation. Int J Mech Sci. 2016;114:217–232.

[28] Barlat F, Brem JC, Yoon JW, et al. Plane stress yield function for aluminum alloy sheets - Part 1: theory. Int J Plast. 2003;19:1297–1319.

[29] Lege DJ, Barlat F, Brem JC. Characterization and modeling of the mechanical behavior and formability of a 2008-T4 sheet sample. Int J Mech Sci. 1989;31:549–563.

[30] Barros PD, Carvalho PD, Alves JL, et al. DD3MAT - a code for yield criteria anisotropy parameters identification. J Phys Conf Ser. 2016.

[31] Banabic D, Aretz H, Comsa DS, et al. An improved analytical description of orthotropy in metallic sheets. Int J Plast. 2005;21:493–512.

[32] Menezes LF, Teodosiu C. Three-dimensional numerical simulation of the deep-drawing process using solid finite elements. J Mater Process Technol. 2000;97:100–106.

[33] Oliveira MC, Alves JL, Menezes LF. Algorithms and strategies for treatment of large deformation frictional contact in the numerical simulation of deep drawing process. Arch Comput Methods Eng. 2008;15:113–162.

[34] Neto DM, Oliveira MC, Menezes LF. Surface smoothing procedures in computational contact mechanics. Arch Comput Methods Eng. 2015;24:37–87.

[35] Menezes LF, Neto DM, Oliveira MC, et al. Improving computational performance through HPC techniques: case study using DD3IMP in-house code. AIP Conf Proc. 2011; 1353, p. 1220–1225.

[36] Hughes TJR. Generalization of selective integration procedures to anisotropic and non-linear media. Int J Numer Methods Eng. 1980;15:1413–1418.